

SENSITIVITY TO HYDROGEN EMBRITTLEMENT OF 2 PIPE STEELS

G Pluinage*¹ and J. Capelle²

*Fiabilité Mécanique. Conseils Silly sur Nied France
ENIM Metz France

* Corresponding author : pluinage@cegetel.net

Fracture toughness and fatigue resistance of two pipe steels (X52 and X70) has been determined using curved specimens (roman tiles) directly extracted from pipes. In both cases, hydrogen embrittlement is done by electrolytic method.

The comparative assessment of local fracture initiation at notches has been done for conditions of electrochemical hydrogenating. The factor of hydrogen concentration in metal was taken into account. The relationship between hydrogen concentration in metal and work for initiation of the local fracture emanating from the notch has been derived. The existence of some critical hydrogen concentration, which causes the significant loss of local fracture resistance of material, was also shown and discussed.

The concept of ΔK_p has been extended to fatigue initiation emanating from notch and under hydrogen embrittlement. Here, fatigue initiation is detected by acoustic emission. It has been found that the fatigue initiation decreases after hydrogen absorption. This can be explained by interaction of hydrogen and plasticity as can be seen for tensile and fracture behaviour steel after introduction of hydrogen.

Keywords : pipe steel, hydrogen embrittlement, local fracture energy, fatigue initiation

1. INTRODUCTION

General reason, which increases of attention to the problem hydrogen degradation of pipeline steels, is fact that hydrogen will play a decisive role in a future energy system, when fossil fuels have become scarce and thus expensive and/or unsuitable from ecological reasons. The number of aspects related to the technical feasibility and economics of developing a hydrogen energy infrastructure are presented and discussed in literature during last decades [1, 2]. The possible use of existing pipeline networks for mixtures of natural gas and hydrogen offers a unique and cost-effective opportunity to initiate the progressive introduction of hydrogen as part of the development of a full hydrogen energy system [3].

From this reason, the safety, durability and integrity issues related to hydrogen/natural gas mixtures in the existing natural gas system become actual and important. First of all, there is a potential problem of so-called "hydrogen embrittlement" of pipeline material - the effects of transported hydrogen on material mechanical properties [4].

Moreover, the specific long-term exploitation of pipelines promotes the hydrogenating of steel. The external environmental conditions cause free corroding processes, where hydrogen can evaluate on metal surface as result of cathodic counterpart of the anodic dissolution reaction. This fact has been proved by several studies [5-7].

External interference incidents are characterised by potentially severe consequences: leaks and ruptures. In majority, these types of incidents are caused by initial damaging of the pipe external surface as result of third party interference e.g. by scratches and gouges and also pitting corrosion.

Such defects can be considered as typical stress concentrators and consequently the privileged sites where the further damaging and failure processes occur.

In this paper, evidence on a critical hydrogen concentration for the ductile brittle transition of two pipe steels X52 and X70 is presented. The strong influence of hydrogen embrittlement on fatigue crack initiation is the second point which focuses our attention.

2. OBJECT OF STUDY AND EXPERIMENTAL PROCEDURE

The objects of study were two API grade pipeline steels, namely: X52 and X70. Nowadays, the steel X52 is the most usable in existed gas pipelines.

The specimens for tests were machined from real pipes (Table 1). The chemical composition of steels and their mechanical properties in air are given in Table 2 and 3 respectively.

Table 1 Size of pipes

Steel grade	Outer diameter D, mm	Wall thickness t, mm
X52	610	11.0
X70	710	12.7

Table 2 Chemical compositions of steels (wt %)

Steel grade	C	Mn	Si	Cr	Ni	Mo	S	Cu	Ti	Nb	Al
X52	0.206	1.257	0.293	0.014	0.017	0.006	0.009	0.011	0.001	<0.03	0.034
X70	0.125	1.68	0.27	0.051	0.04	0.021	0.005	0.045	0.003	0.033	0.038

Table 3 Mechanical properties of steels in air at ambient conditions

Steel grade	σ_U, MPa	σ_Y, MPa	Elongation. %
X52	528	410	30.2
X70	712	590	18.3

For tests (fatigue and fracture), the special “Roman tile” [8] specimens were used. The specimens were notched for modelling of the longitudinal external defects under operating internal pressure. The specimen view and notch geometry are given in Fig. 1. The study was conducted in special soil solution NS4 with $pH=6.7$ [9]

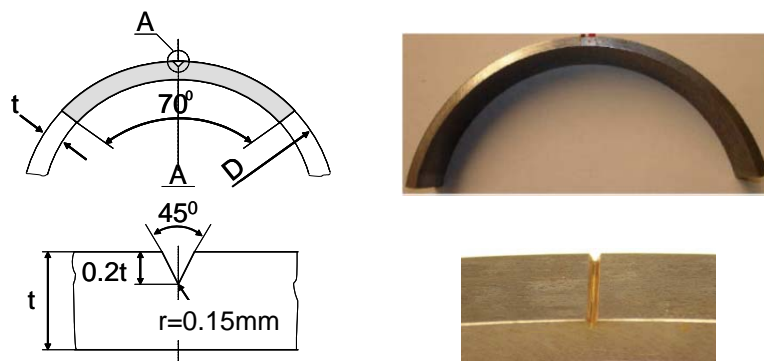


Fig. 1 “Roman tile” specimen and geometry of notch

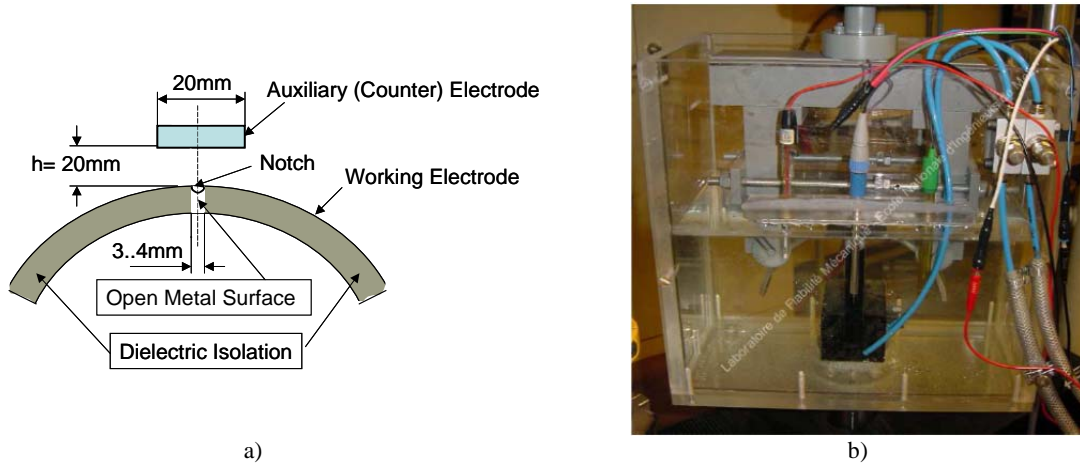


Fig. 2 Mutual location of working electrode (specimen) and auxiliary (counter) electrode (a) and general view of corrosion cell (b)

The specimens were coated by special dielectric isolation, excepting the small area at the notch (Fig. 3). The size of auxiliary (counter) electrode was 20x40 mm. In this case its square is significantly larger than the working electrode area, which to be polarised. During testing the specimens were immersed into the cell with NS4 solution (Fig. 2) and exposed under constant potential of cathodic polarisation $E_{cath} = const$. For this experimental procedure the Potentiostat VMP has been used. During all test the level of pH was controlled and regulated between 6.6 and 6.7 by bubbling of CO_2 gas.

In given tests, the specimens were hydrogen charged at some constant potential of polarisation, which is slightly negative than free corrosion potential for the given steels. Taking into account that for studying steels the free corrosion potential is about $E_{corr} = -800mV(SCE)$, it has been chosen. Moreover, for simulating of the service conditions, the specimens were loaded during the hydrogen-charging process. The level of load was defined as the gross hoop stress $\sigma_{gross} = 194$ and 195.7 MPa respectively which corresponds of the internal pressure in pipe under exploitation $p_{exp} = 70$ bar

The hydrogen-charging process was controlled by registration of the cathodic polarisation current $I_{cath}(\tau)$. The total quantity of evaluated hydrogen on metal surface during time of exposition τ_{exp} can be found as:

$$Q_H^{ev} = \int_0^{\tau_{exp}} I_{cath}(\tau) d\tau \quad \text{under } E_{cath} = const. \quad (1)$$

Hydrogen concentration in metal has been determined on the base of hydrogen discharging process under anodic polarisation with using of hydrogen electrochemical oxidation method proposed in work [10]. For this aim, the standard three-electrode electrochemical cell has been used. The hydrogen discharging of specimen was carried out in 0.2 M NaOH ($pH=12.4$) solution under anodic polarisation $E_{anodic} = +168mV(SCE)$ during some defined time τ_{dis} . The total quantity of absorbed hydrogen by metal can be defined as:

$$Q_H^{abs} = \int_0^{\tau_{dis}} [I_H(\tau) - I_{ref}(\tau)] d\tau \quad \text{under } E_{anodic} = const. \quad (2)$$

Here $I_H(\tau)$ is anodic polarisation current for hydrogen charged specimen and $I_{ref}(\tau)$ is anodic polarisation current for specimen without hydrogen (reference curve). Calculation of hydrogen concentration was done according to formula:

$$C_H = \frac{Q_H^{abs}}{zFv}. \quad (3)$$

Where z is the number of electrons take in reaction; F is the Faraday constant; v is the effective volume of specimen: C_H [mol/cm³]; Q_H^{abs} [A·s]; $z = 1$; $F = 9,65 \cdot 10^4$ C/mol.

After assigned exposition under hydrogenating conditions, all specimens were tested to failure under increasing static loading or fatigue according to 3-point bending scheme. The “load – displacement” diagram and acoustic emission (AE) signals were simultaneously registered by PC during the tests. The start of fracture process has been defined by acoustic emission method.

3. RESULTS AND DISCUSSION

Process of hydrogen charging of pipeline steels at the given conditions of cathodic polarisation was characterised by following parameters: averaged meaning of cathodic current density i_c ; total quantity of evaluated Q_{ev} and absorbed Q_{abs} hydrogen; coefficient of efficiency of hydrogen permeation in metal $k = Q_{abs}/Q_{ev}$ and hydrogen concentration in metal C_H . It can be seen that for assigned testing conditions, i.e. in deoxygenated, near-neutral pH NS4 solution and under loading by tensile stress, which simulates of operating conditions, the resistance to hydrogen absorption decreases with decreasing of steel strength.

Based on received experimental results, the hydrogen concentration in given steels versus time of exposition of specimens in the hydrogenating conditions can be described by power relation:

$$C_H = A \cdot 10^{-6} \cdot \tau^m. \quad \left[\text{mol/cm}^3 \right]. \quad (4)$$

Where A and m are constants (see Table 4).

Table 4 Meanings of constants in formula (4)

Steel	A	m
API X52	0.30	0.57
API X70	0.40	0.42

3.1 Local strength

The study of local strength of notched specimens in presence of hydrogen was resulted in the dependencies of total work U_i for initiation of the local fracture emanating from the notch. The scheme of determination of parameter U_i is presented in Fig. 3

$$U_i = \int_0^{\Delta_i} P(\Delta) \cdot d\Delta. \quad (5)$$

Here the hydrogen concentration C_H in metal was calculated by using of the analytical relation (4). The main observation based on these results is the existence of some critical time of exposition and as a consequence – some critical hydrogen concentration C_H^* , when the essential

decreasing of fracture toughness value is occurred (Fig. 3). The values of C_H^* for studied steels are given in Table 5.

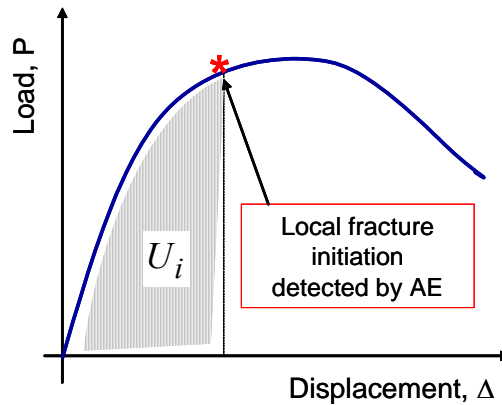


Fig 3. Scheme of determining of work for local fracture initiation

Table 5 Critical hydrogen concentrations C_H^* for API grade pipeline steels

Steel	$C_H^*, 10^6 \text{ mol/cm}^3$
X52	4.3
X70	2.3

The steel X70 demonstrates very high sensitivity to notch effect even in air and the presence of hydrogen strengthens this tendency. The hydrogen concentration about $C_H^* \approx 2.3 \cdot 10^{-6} \text{ mol/cm}^3$ can be considered as critical, because at this conditions the given steel losses in 2.5 times its local strength with comparison of test in air. Therefore, for assigned testing conditions, steel X52 is preferable than steel X70 from the point of view of local strength at notches under hydrogen embrittlement.

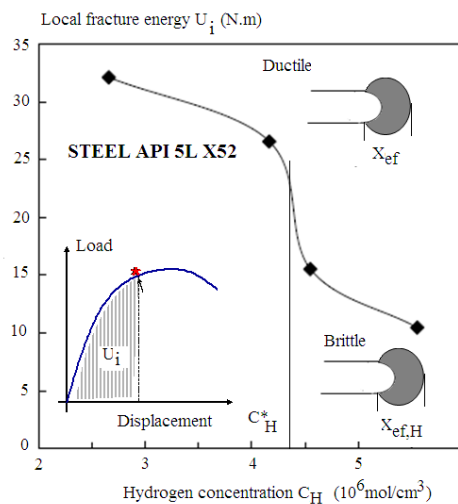


Fig .4 Ductile-brittle transition with hydrogen concentration in API5L X52 steel.

This critical hydrogen concentration at ductile brittle transition can be explained by a competition to the fracture process volume and the hydrogen affected fracture process volume. In an area approach, the effective distance X_{ef} represents the diameter of the fatigue process zone assumed as

cylindrical. Its determination is based on a procedure involving the relative stress gradient to determine an inflexion point on the notch tip opening stress distribution [8]. If X_{ef} is smaller than $X_{ef, H}$, the corresponding value after hydrogen embrittlement, the effective stress in the fracture process volume is greater and then the work done for fracture is higher.

There is the tendency of monotonic decreasing of C_H^* values with increasing of yield stress σ_Y or ultimate stress σ_U steel (Fig. 10). This dependency can be described by power function, like to:

$$C_H^* = B_1 \cdot (\sigma_Y)^{n_1} \text{ or } C_H^* = B_2 \cdot (\sigma_U)^{n_2}, \quad (6)$$

where B_1, B_2, n_1, n_2 are the some constants of material's properties and testing conditions. Here, the standard deviation $R^2 = 0.98-0.99$ that is fully acceptable. As first approximation, it can be concluded that

$$C_H^* \sim \frac{1}{\sigma_U^2}. \quad (7)$$

3.2 fatigue initiation

The fatigue resistance to initiation of the API 5L X52 and X70 steels has been measured in radial direction at room temperature using non-standard curved notched specimens, namely, "Roman tile" specimens because the pipe dimensions do not permit to measure through thickness mechanical characteristics.

The applied load, frequency and the fatigue cycle (sinusoidal) were monitored on the control panel. Hydrogen charging was made using the same cell filled with NS4 solution. Tests conditions are given in Table 6.

Table 6 : Fatigue test conditions

Shape of the cycle used	Sinus:
Frequency :	0.05 Hz
Load ratio	0.5
Working potential	- 1 V _{sce}
Electrolytic solution	New Solution 4 (NS4)
Solution pH	between 6.66 and 6.74

Wöhler curves were drawn at both initiation and failure. Results are presented in a bi logarithmic graph of stress amplitude versus number of cycles to failure. The classical power fit of the stress range versus the number of cycles to failure is in accordance with Basquin's law:

$$\Delta\sigma = \sigma'_f (N_R)^b \quad (8)$$

where σ'_f is the fatigue resistance and b the Basquin's exponent. Results are presented in Table 7.

Table 7: Fatigue resistance parameters with and without hydrogen charging for X 52and X70 steels

Steel, environment	σ'_f fatigue resistance (MPa)	exponent β	R^2
X70 air	436	-0.023	0.94
X70 Hydrogen	395	-0.015	0.94
X52 air	343	-0.022	0.89
X52 Hydrogen	301	-0.012	0.95

Fatigue phenomenon consists of two parts, fatigue initiation and crack propagation until failure. When using optical devices, definition of initiation depends on optical resolution of the equipment. In our tests, we detect fatigue initiation by acoustic emission which is more sensitive than optical method. Acoustic emission is registered during test by two sensors. Fatigue initiation is easily detected by an energy burst. This method is also reliable and gives supplementary information on fatigue mechanism. Stress range versus number of cycles to initiation is fitted by a power law similar to Basquin's one.

$$\Delta\sigma = \sigma'_i (N_i)^\beta \tag{9}$$

where σ'_i is fatigue initiation resistance and β an exponent. $\Delta\sigma$ is the gross stress range.

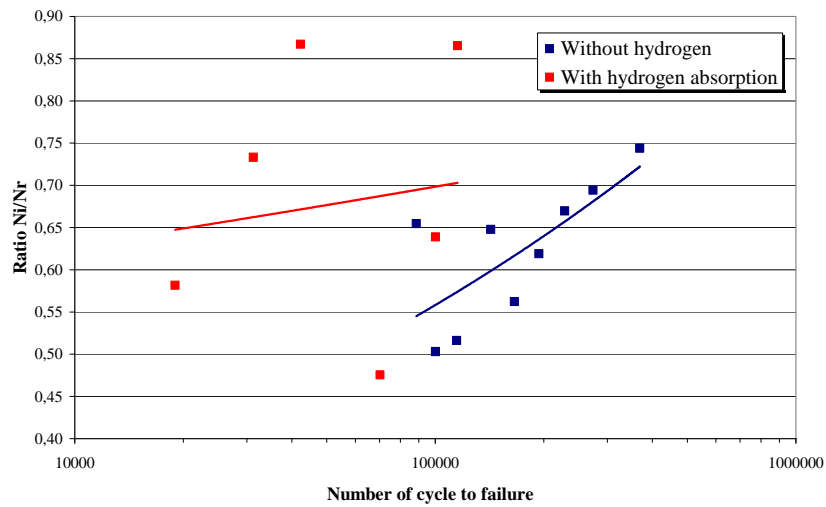


Figure 5: Evolution of ratio N_i/N_r versus number of cycles to failure for X52 steel.

Table 8: Fatigue initiation resistance parameters with and without hydrogen charging for X 52and X70 steels

Steel, environment	σ'_i fatigue initiation resistance (MPa)	Exponent β	R^2
X70 air	395	-0.016	0.96
X70 Hydrogen	368	-0.010	0.97
X52 air	325	-0.018	0.90
X52 Hydrogen	296	-0.011	0.95

Evolution of ratio N_i/N_r versus number of cycles to failure is plotted in Figure 6. We note that fatigue crack propagation is faster in presence of hydrogen because the difference $N_r - N_i$ is strongly reduced.

Barsom and McNicol [11], Jack and Price [12], Clark [13] and Truchon [14] have used the parameter $\Delta K/\sqrt{\rho}$ to express fatigue resistance on notched specimens. Boukharouba et Al [15] have compare fatigue initiation criteria with a criterion based on the elasto plastic notch stress intensity factor K_p on welded specimen made in low strength steel. The same parameter has been used to plot a fatigue initiation curve $K_p (= f(N_i))$. One notes that this curve are not sensitive to pipe steels but sensitive to environment.

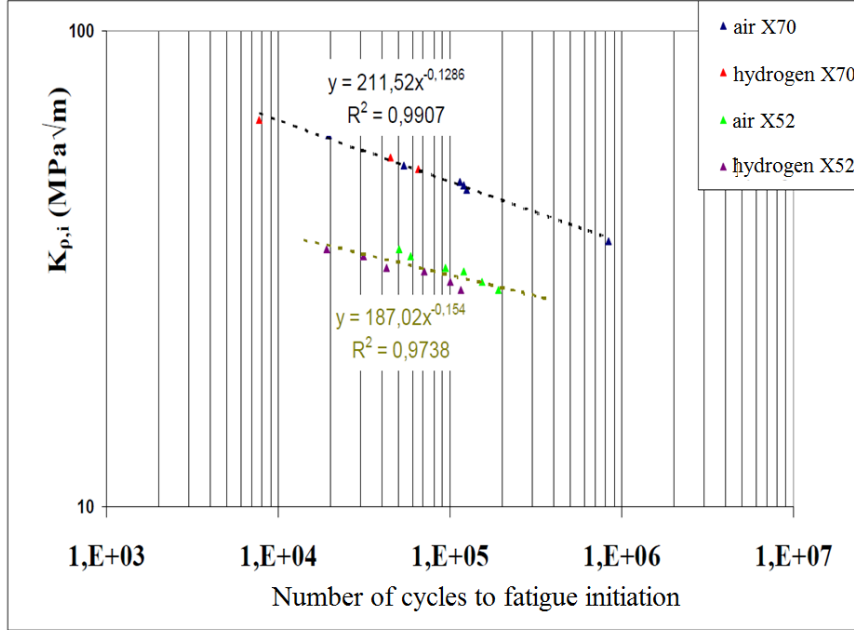


Figure 6 : Fatigue initiation curves for both steels with and without hydrogen embrittlement.

The hydrogen concentration increases as a power function of time (see equation 4) and then depends on number of cycles to initiation N_i and test frequency f . The local hydrogen concentration depends on hydrostatic stress σ_h . The average hydrogen concentration is the local one computed over the effective distance V_{ef} :

$$\bar{C}_H = \frac{1}{X_{ef}} \int_0^{X_{ef}} A \left(N_i \times \frac{1}{f} \right)^m \cdot \exp \left[-\frac{V_H \cdot \sigma_h(r)}{R \cdot (T - T_0)} \right] dr \quad (10)$$

Where A and m are constants of equation 4, R Perfect gas constant, V_H molar hydrogen volume.

Notch Stress Intensity Factor is given according to [8] :

$$K_{\rho,air} = \sigma_{ef} \cdot \sqrt{2\pi \cdot X_{ef}} \quad (11)$$

In hydrogen, NSIF takes the following form because maximum hydrogen concentration is localised at peak stress

$$K_{\rho,H} = \sigma_{\max,H} \cdot \sqrt{2\pi \cdot X_{ef,H}} \quad (12)$$

Effective stress σ_{ef} , peak stress $\sigma_{\max,H}$, effective distance X_{ef} and effective distance under hydrogen concentration $X_{ef,H}$ are obtained by computing notch tip stress distribution by finite element and using stress strain behavior with and without hydrogen embrittlement respectively.

A plot of the following ratios $\left(\frac{\sigma_{\max,H}}{\sigma_{ef}} \right)$ and $\left(\frac{X_{ef,H}}{X_{ef}} \right)$ indicates an exponential dependence with average hydrogen concentration.

$$\sigma_{\max,H} = \sigma_{ef} \cdot \exp(A_1 \cdot \bar{C}_H + B_1); X_{ef,H} = X_{ef} \cdot \exp(A_2 \cdot \bar{C}_H + B_2) \quad (13)$$

$$\begin{cases} A_1 = -9 \cdot 10^{-5} & B_1 = 0,1182 \\ A_2 = -5 \cdot 10^{-4} & B_2 = -0,0442 \end{cases}$$

So the Notch Stress Intensity factor under hydrogen can be expressed as a function of K_{ρ} , air

$$K_{\rho,H} = K_{\rho,air} \cdot f(\bar{C}_H, \alpha) \quad (14)$$

$$\text{With } f(\bar{C}_H) = \exp\left[\left(A_1 + \frac{1}{2}A_2\right) \cdot \bar{C}_H + \alpha \cdot \left(B_1 + \frac{1}{2} \cdot B_2\right)\right]$$

The parameter α is introduced in order to get $K_{\rho,H} \rightarrow K_{\rho,air}$ when $\bar{C}_H \rightarrow 0$

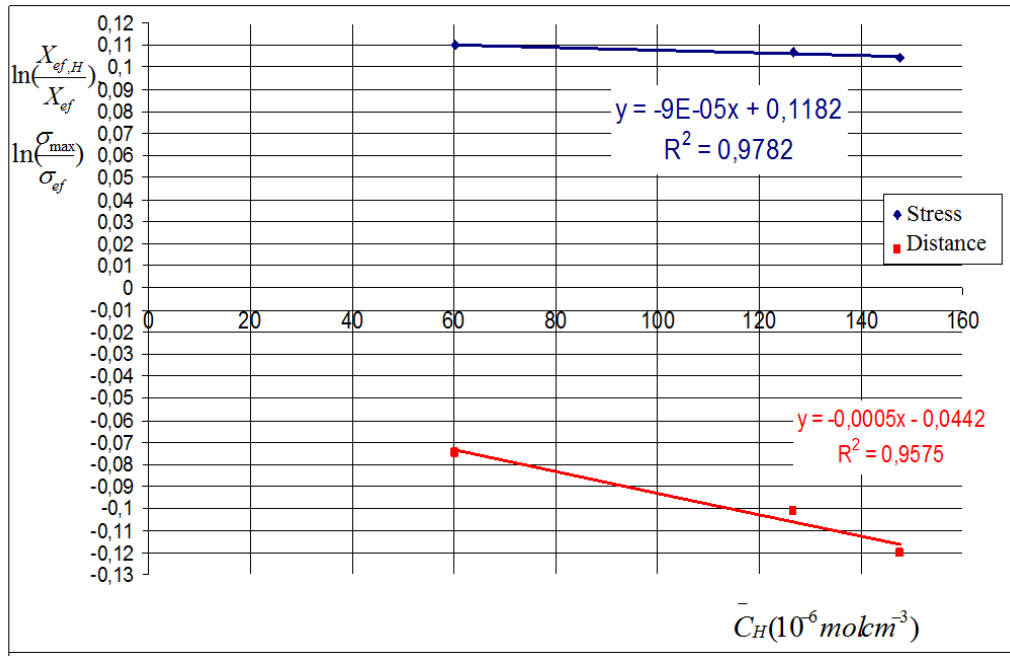


Figure 7 : Evolution of ratios $\left(\frac{\sigma_{\max,H}}{\sigma_{ef}}\right)$ and $\left(\frac{X_{ef,H}}{X_{ef}}\right)$ with average hydrogen concentration.

4. CONCLUSION

It is important to note that hydrogen concentration provides a fracture resistance transition .similarly to temperature, loading rate and notch acuity in pipe steels X52 and X. This phenomenon is describes for the first time (according to our knowledge) in this paper.

Some critical hydrogen concentration C_H^* exists for tested steels, which causes the significant loss of local fracture resistance of material at notches. The tendency of monotonic decreasing of C_H^* values with increasing of yield stress σ_Y or ultimate stress σ_U of steels has been derived.

Critical hydrogen concentration C_H^* may be considered as an important engineering parameter for forecasting of strength and reliability of exploited pipelines and under designing of new pipelines for hydrogen transportation as well.

Hydrogen embrittlement reduces fatigue life by increasing fatigue crack propagation and reducing number of cycles to initiation. Fatigue initiation can be described by the Notch Stress Intensity Factor which is sensitive to average hydrogen concentration.

References

- [1]. Mulder G., Hetland J. and Lenaers G. Towards a sustainable hydrogen economy: Hydrogen pathways and infrastructure. *International Journal of Hydrogen Energy*, 32, Issues 10-11 (2007) 1324-1331
- [2]. Wietschel M., Hasenauer U. and de Groot A. Development of European hydrogen infrastructure scenarios - CO₂ reduction potential and infrastructure investment. *Energy Policy*, 34, Issue 11 (2006) 1284-1298
- [3]. NaturalHy Project, <http://www.naturalhy.net>
- [4]. Hanneken J. W. Hydrogen in metals and other materials: a comprehensive reference to books, bibliographies, workshops and conferences. *International Journal of Hydrogen Energy*. 24, No 10. (1999) 1005-1026.
- [5]. Cheng Y.F. Fundamentals of hydrogen evolution reaction and its implications on near-neutral pH stress corrosion cracking of pipelines. *Electrochimica Acta* 52 (2007) 2661–2667
- [6]. Dey S., Mandhyan A.K., Sondhi S.K., Chattoraj I. Hydrogen entry into pipeline steel under freely corroding conditions in two corroding media. *Corrosion Science* 48 (2006) 2676–2688
- [7]. Shipilov S.A., May I.L. Structural integrity of aging buried pipelines having cathodic protection. *Engineering Failure Analysis* 13 (2006) 1159–1176
- [8]. Adib-Ramezani H., Jeong J., Pluvinage G. Structural integrity evaluation of X52 gas pipes subjected to external corrosion defects using the SINTAP procedure. *International Journal of Pressure Vessels and Piping* 83 (2006) 420–432
- [9]. Capelle J., Gilgert J., Dmytrakh I., Pluvinage G. Sensitivity of pipelines with steel API X52 to hydrogen embrittlement. *International Journal of Hydrogen Energy* 33 (2008) 7630-7641
- [10]. Yan M., Weng Y. Study on hydrogen absorption of pipeline steel under cathodic charging. *Corrosion Science* 48 (2006) 432–444
- [11]. M. Barsom and R. C. McNicol, Effect of stress concentration on fatigue-crack initiation in HY-130 steel. *ASTM STP* 559, 183-204 (1974).
- [12]. A. R. Jack and A. T. Price, The initiation of fatigue cracks from notches in mild steel plates. *Int. J. Fracture Mech.* 6 (4) (1970).
- [13]. W. G. Clark, Jr, Evolution of the crack initiation properties of type 403 stainless steel in air and steam environment. *ASTM STP* 559, 205-224 (1974).
- [14]. M. Truchon, Amorçage de fissures en fatigue à partir d'entaille, application aux joints soudés. *Bulletin Technique du Bureau Veritas* 67 (5) (1985).
- [15]. Boukharouba, T. Tamine, L. Niu, C. Chehimi and G. Pluvinage The use of notch stress intensity factor as a fatigue crack initiation parameter. *Engineering Fracture Mechanics* Vol. 52, No. 3, pp. 503-512, (1995).